Article accepted in the Don L. Anderson honor volume published jointly by
the Geological Society of America and the American Geophysical Union
Editors: Gillian R. Foulger (Durham Univ), Michele Lustrino (Univ. Rome) & Scott King (Virginia Tech.)

Lithospheric structure of the Atakor metacratonic volcanic swell (Hoggar, Tuareg Shield, Southern Algeria): Electrical constraints from magnetotelluric data.

Abderrezak Bouzid*

Boualem Bayou

CRAAG, Route de l'Observatoire, BP 63 Bouzaréah, Algiers, 16340, Algeria

Jean-Paul Liégeois

Geodynamics and Mineral Resources, Royal Museum for Central Africa, B-3080 Tervuren, Belgium

Seid Bourouis

Sofiane Saïd Bougchiche

Abdelhamid Bendekken

Abdeslam Abtout

Walid Boukhlouf

CRAAG, Route de l'Observatoire, BP 63 Bouzaréah, Algiers, 16340, Algeria

Aziouz Ouabadi

Laboratoire de Géodynamique, Géologie de l'Ingénieur et Planétologie, FSTGAT/USTHB, BP 32, El-Alia Bab Ezzouar, Algiers, 16111 Algeria

**E-mail: a.bouzid@craag.dz*

ABSTRACT

The Tuareg Shield, to which Hoggar belongs, has a swell-shaped morphology of lithospheric scale of c. 1,000 km in diameter linked to Cenozoic volcanism occurring in several regions, including Atakor, the center of the swell, up to nearly 3,000 m in altitude. The lack of high-resolution geophysical data for constraining its deep structure is at the origin of a controversy about its innermost nature and about the origin of the Cenozoic volcanism. During the course of this study, magnetotelluric (MT) broadband data were collected at 18 sites forming a NE-SW profile 170 km long, within the Atakor region. The electrical resistivity model obtained by inverting the magnetotelluric data reveals lithospheric structure down to a depth of about 100 km. From this depth to the surface, the model does not show any regional anomaly that may result from a metasomatized lithosphere or from an asthenospheric upwelling, including a mantle plume. MT data reveal rather a lithosphere affected by a set of rather thin subvertical conductors that can be attributed to the electrical signature of some known shear zones resulting from the Pan-African evolution of the LATEA metacraton, which globally corresponds to the uplifted Central Hoggar swell. The main anomaly is deeply rooted in the

lithosphere and underlies remarkably the Atakor/Manzaz volcanic districts. As a whole, MT data are therefore properly integrated within the hypothesis of the reactivation of shear zones due the intraplate deformation related to the collision between Africa and Europe since the Eocene applied on a metacratonic region.

Keywords: Tuareg shield, metacraton, Atakor volcanic district, lithospheric structure, magnetotellurics

INTRODUCTION

In Central Sahara, the Hoggar massif in southern Algeria together with the Adrar of Iforas in northern Mali and Aïr in northern Niger form the Tuareg shield, 500,000 km² of mainly Precambrian lithologies (Fig. 1). The Tuareg shield formed during the Neoproterozoic convergence of several old Archean-Paleoproterozoic continents (including Central Hoggar) and intervening oceanic terranes, leading eventually to the formation of Gondwana (Meert and Lieberman, 2008 and references therein). After several accretions of oceanic terranes (0.87-0.63 Ga), the main Pan-African intercontinental collision (0.63-0.58 Ga) between the West African craton and the Saharan metacraton (Fig. 1) generated a general northern tectonic escape of the Tuareg terranes (Black et al., 1994; Liégeois et al., 2003; Abdallah et al., 2007; Liégeois et al., 2013 and references therein). This Pan-African escape collision dissected the old Central Hoggar continent through the reactivation of preexisting mega-shear zones, which allowed the emplacement of granitoid batholiths (Acef et al., 2003; Liégeois et al., 2003). This process, which induced no important lithospheric thickening, corresponds to a metacratonic evolution (Liégeois et al., 2013). The result in Central Hoggar is the juxtaposition of four terranes mostly comprising Archean and Paleoproterozoic lithologies reactivated during the Pan-African orogeny that induced relative displacement of several hundreds of km and the emplacement of granitoids, but leaving largely intact large tracts of pre-Pan-African rocks (Liégeois et al., 2003; Bendaoud et al., 2008). These four terranes (Laouni, Azrou n'Fad, Tefedest, Egéré-Aleksod) gave its name to the LATEA metacraton (Fig. 1) in order to witness the globally similar behavior of these terranes, even if displaced (Liégeois et al., 2003). It is within the LATEA metacraton that most of the Hoggar Cenozoic volcanism was emplaced (Dautria et al., 1988; Aït-Hamou et al., 2000; Liégeois et al., 2005). Although the origin of this volcanism is still debated, various authors conclude that the rise of magma occurs through fracture zones that affect the lithosphere of Hoggar (Aït-Hamou et al., 2000; Liégeois et al., 2005; Azzouni-Sekkal et al., 2007). The origin of the present morphology of the Hoggar swell is also under discussion: it is interpreted as the isostatic response of a light upper mantle resulting from an asthenospheric rise (Crough,

1981; Lesquer et al., 1988; Beccaluva et al., 2007), either caused by the arrival of a mantle plume (Aït-Hamou et al., 2000) or as the result of the combination of edge-driven convection

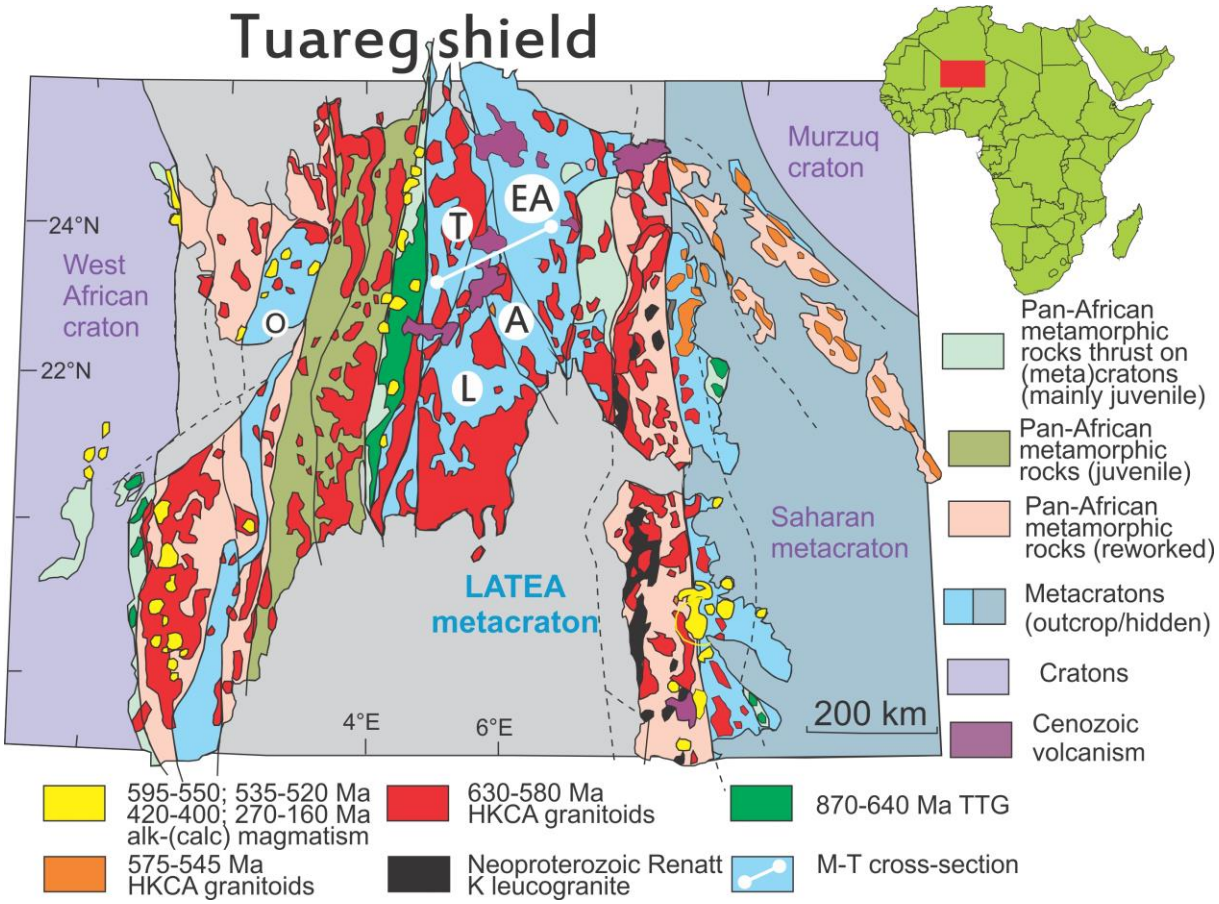

Fig. 1: A simplified geologic map of the Tuareg shield (modified from Bertrand & Caby, 1977; Black et al., 1994; Liégeois et al., 1994; 1998; 2003; Fezaa et al., 2010). L= Laouni, A= Azrou n'Fad, T= Tefedest, EA= Egéré-Aleksod, the four terranes forming the LATEA metacraton. O= In Ouzzal Archean granulitic terrane. The magnetotelluric section studied here is indicated by the white line.

with far-field lithospheric buckling due to Africa-Europe collision inducing the slowdown of the African plate and its intraplate deformation (Liégeois et al., 2005; Rougier et al., 2013).

High-resolution geophysical data are of paramount importance for constraining the deep structure and dynamics of the continental lithosphere. The goal of this study is to constrain the deep structure of Central Hoggar, characterized by a major intracontinental swell and recent volcanism, by using electrical conductivity. Magnetotellurics (MT) is a passive geophysical technique that is sensitive to the distribution of electrical conductivity in the crust and upper mantle. Magnetic field and telluric current fluctuations in time induced by atmospheric electrical activity (lightening) and ionospheric currents are measured at the Earth surface. In a simple one-dimensional Earth, the ratio of an electric field component to the magnetic field orthogonal component allows inferring the electrical conductivity of the crust and upper mantle (Tikhonov, 1950; Cagniard, 1953). This scalar relationship is extended to a tensor relationship for two-dimensional or three-dimensional Earth. The

penetration depth of the technique is proportional to the square root of the oscillation period length of the electromagnetic wave.

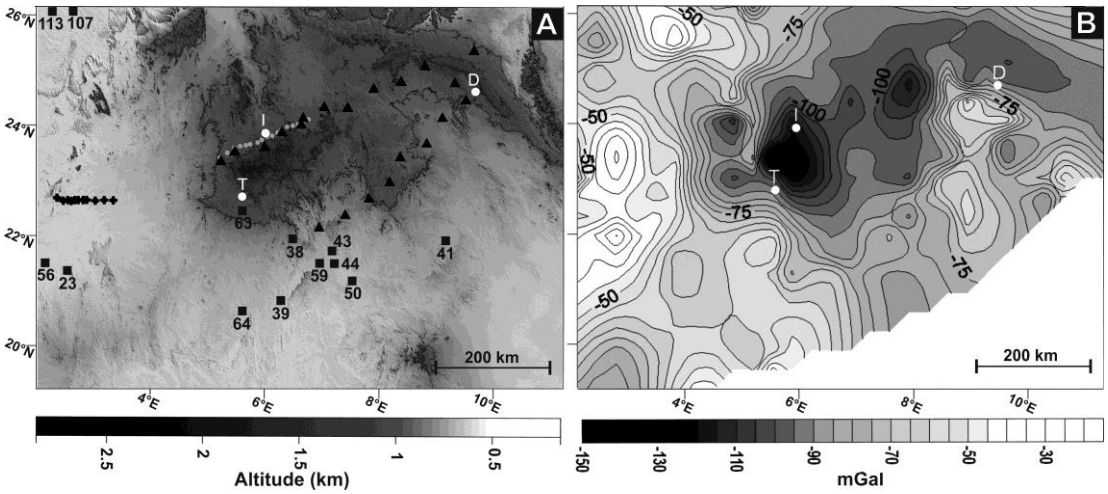

Fig. 2. A: Topographic map of the Atakor area. The black squares represent the measurement points of heat flow values in mW/m2 (from Lesquer et al., 1988). The white circles, the three cities: T= Tamanrasset, I= Ideles and D= Djanet. White dots represent MT stations used in this study. The black triangles represent the regional study of Bouzid et al. (2004) and black crosses those of Bouzid et al. (2008). In B, the Bouguer anomaly map of the same area as in A, (from Lesquer et al., 1989, modified).

Temperature increase, presence of melt, fluid phase or minerals, even in small amounts, affects, variably, the electrical conductivity of the crust and upper mantle (Shankland and Ander, 1983; Jödicke, 1992; Jones, 1999; Nover, 2005). Faults and shear zones, such as those affecting the lithospheric structure of the Hoggar shield, are generally associated with an increase of the conductivity even if some faults may not have detectable electrical signature (Jones et al., 1992; Wu et al., 2002; Unsworth and Bedrosian, 2004). In Western Hoggar, the shear zones limiting the In Ouzzal Archean metacratonic terrane (Fig. 1; Adjerid et al., 2008) from the adjacent Pan-African terranes to the west and east, are associated with a sharp increase in the electrical conductivity (Bouzid et al., 2008). In the Deccan Volcanic Province, magnetotelluric data revealed a crust composed of several resistive blocks separated by conductive structures showing good correlation with crustal faults (Harinarayana et al., 2007). In the Damara Belt, magnetotellurics also reveals the existence of subvertical conductors corresponding to major shear zones. This increase in conductivity was attributed to an enrichment or precipitation from graphite-bearing fluids due to shear zone reactivations during the late Pan-African period (Ritter et al., 2003). In the Northern Basin and Range region (western USA), magnetotelluric data highlight an important electrical resistivity decrease in the lower crust and in the uppermost mantle: it was interpreted there as the result of a magma underplating around the Moho discontinuity that released hydrothermal fluids (Wannamaker et al., 2008; Meqbel et al., 2014).

This study is focused on the center of the Hoggar shield, close to the top of the Hoggar topographic swell, where altitudes of the Precambrian basement reach 1,000 to 1,500 m

(Figs. 1, 2). This is the locus of two of the largest volcanic districts of the Hoggar, namely Atakor and Manzaz (Fig. 3).

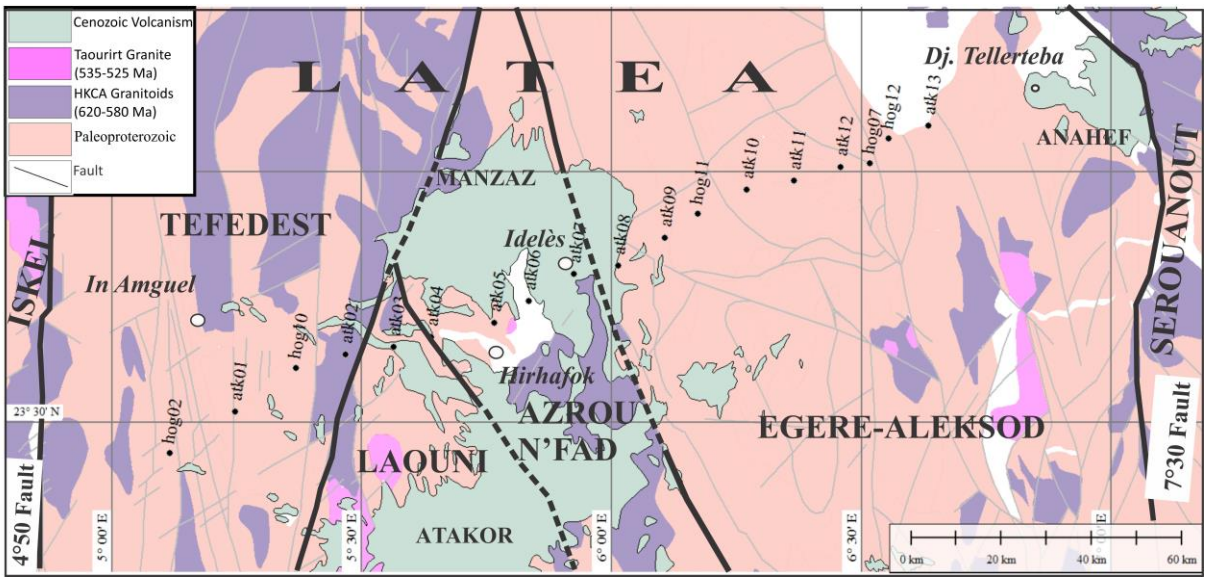

Fig. 3: A simplified geologic map of the study area (modified from Bertrand and Caby, 1977), the terrane boundaries (shear-zones; heavy lines) are from Black et al. (1994), Liégeois et al. (2003) and Azzouni-Sekkal et al. (2007). Black dots are MT stations (hog: 1993 and 2003 surveys; atk: 2012 survey); White circles are cities.

GEOLOGICAL AND GEOPHYSICAL SETTINGS

The LATEA metacraton corresponds geographically to the Central Hoggar. Built during the Eburnean orogeny (2.0 – 1.9 Ga; Peucat et al., 2003; Bendaoud et al., 2008), it acquired a thick and rigid lithospheric mantle during the Mesoproterozoic which led to its cratonization (Liégeois et al., 2003). However, during the Pan-African orogeny, LATEA underwent a metacratonization process (Abdelsalam et al., 2002; Liégeois et al., 2013), being squeezed between the nearly opposed pushing of the West African craton and the Saharan metacraton during the general tectonic escape to the north of the Tuareg shield terranes (Black et al., 1994). During that process, LATEA was dissected into four terranes through the reactivation of mega-shear zones underlain by linear lithospheric delamination, the whole allowing the intrusion of high-K calc-alkaline batholiths and of late shallow depth alkali-calcic plutons during the 630-580 Ma period (Acef et al., 2003; Liégeois et al., 2003; Abdallah et al., 2007).

During the Cenozoic, the LATEA metacraton concentrated the volcanic activity present in the Hoggar Shield. This volcanism started at the end of the Eocene (c. 35 Ma) in the Anahef district with tholeiitic flood basalt 700 m thick (Ait-Hamou et al., 2000) intruded by subvolcanic ring complexes (Tellerteba ring complex, 35 Ma; Rossi et al., 1979; Achkal complex, 29 Ma; Maza et al., 1998) finally capped by 24 Ma-old alkaline rhyolites, indicating uplift rates of ~0.4 mm/year (Maza et al., 1998). Three later volcanic episodes (basalts and trachytes, few phonolites and rhyolites) occurred in several districts during the Miocene (20-

12 Ma), Mio-Pliocene (8.5-4 Ma) and in minor amounts during the Quaternary (Liégeois et al., 2005 and references therein). In the studied area, volcanism occurred in two volcanic districts, Atakor (2150 km2) and Manzaz (1500 km2). Together, they represent about 425 km³ of lavas, which represents between 18 and 27% (depending of the estimated volume for the Anahef flood basalts) of all the lavas emitted during the Cenozoic in Hoggar (Liégeois et al., 2005). More precisely in the Atakor district, the most important volcanic activity occurred during the 20-12 Ma period (Burdigalian-Serravalian) with additional activities during the Messinian-Zanclean (6.7-4.2 Ma) and during the Gelasian-Holocene (1.95-0.01 Ma; Azzouni-Sekkal et al., 2007). Let us remark that intervening quiescence periods were marked by tectonic activity (Azzouni-Sekkal et al., 2007).

The Hoggar swell, associated with the above described volcanism, has a diameter of 1,000 km and a mean altitude of 1,200 m with the basement attaining an altitude of 2,400 m (Fig. 2), the highest points being of volcanic nature with the very highest one being the phonolitic Mount Tahat at 2,918 m (Rougier et al., 2013). The existence of Cretaceous deposits resting directly on the Precambrian basement of the Hoggar led to the thinking that a first rising of the shield occurred prior to the Cretaceous (Liégeois et al., 2005). Apatite (U-Th)/He thermochronological data and apatite fission track data indicate that the current swell uplift began during the Eocene before the first volcanic activity at c. 35 Ma (Rougier et al., 2013). This is in agreement with the modeling of river profiles applied to some Hoggar wadis, which suggest that uplift started in the lower Eocene (40-50 Ma; Roberts & White, 2010).

Geophysical data are scarce but bring important constraints. (1) The studied area, and more generally the LATEA metacraton, is located at an end of the negative gravity anomaly reaching -120 mgal (Fig. 2) that was modeled to be related to a light body in the lithosphere (between 20 and 70 km depth with a maximum thickness of 30 km; Lesquer et al., 1988); (2) The Hoggar shield as a whole does not show any thermal anomaly, the average observed heat flow being 53 mW/m2 with a local value of 63 mW/m2 obtained in southern Atakor (Fig. 2; Lesquer et al., 1989). This led Ayadi et al. (2000) to consider that small high-temperature mantle bodies may intrude the crust beneath the recent volcanic areas; (3) At the scale of the African continent, the surface wave tomography, with several hundred km lateral resolution, shows no particular upper mantle seismic signature beneath Hoggar (Sebaï et al., 2006), except that its lithosphere is thinner than the adjacent West African craton and Murzuq craton (Fishwick and Bastow, 2011; Liégeois et al., 2013). Seismic tomography data of higher resolution obtained at local scale shows that Atakor and Tahalgha volcanic districts are underlined by a crust and upper mantle with low P-wave velocity (Ayadi et al., 2000); (4) Small scale variations in the lithospheric structure and characteristics around the Tamanrasset Geoscope station (Fig. 2) were obtained by an analysis of receiver functions (Liu and Gao, 2010); the authors deciphered differences in lithospheric mechanical

characteristics between Laouni and Tefedest terranes, which could explain the presence of volcanism in the latter and its absence in the former; moreover, they estimated the crustal thickness to 34 km at local scale, while different estimates give a thickness in the range of 34 to 40 km (Merlet, 1962; Sanvol et al., 1998; Hazler et al., 2001; Pasyanos and Walter, 2002; Gangopadhyay et al., 2007); (5) Magnetotelluric reconnaissance profiles carried out in Hoggar with relatively low lateral resolution (distance between stations of 40-50 km), show no regional conductivity anomalies (Bouzid et al., 2004).

MAGNETOTELLURIC DATA COLLECTION

The magnetotelluric (MT) data described here come from three field surveys carried out in 1993, 2003 and 2012. They comprise data collected from five stations during two earlier field surveys carried out in 1993 and 2003, for the reconnaissance of the whole geological structure of the Hoggar, prefixed with “hog” and data collected in April 2012 from 13 new sites, called atk01 to atk13. The consequent 18 MT sites form a NE-SW profile that is 170 km long, centered on the town of Ideles which is located 150 km NE of Tamanrasset (Fig. 3). The SW end of the profile is located to the south of In Amguel and its NE end is located near Adrar Tellerteba (Figs. 1, 3).

This magnetotelluric profile extends on the four terranes constituting the LATEA metacraton (Fig. 3): from SW to NE, Tefedest (4 MT sites), Laouni (2 MT sites), Azrou n’Fad (3 MT sites) and Egéré-Aleksod (9 MT sites). In addition, the MT profile passes between the two Cenozoic volcanic massifs of Manzaz to the north and Atakor to the south (Fig. 3), through the Hirafok and Ideles localities. The inter-station distance of c. 10 km was chosen for improving significantly the lateral resolution of the geoelectric model beneath the study area. For obtaining deep penetration within the geological structure, the time series of the natural electromagnetic field for the newer 13 sites (atk01 to atk13) were recorded during about 20 hours at each site using a V5 System 2000® of Phoenix Geophysics. Two electrode pairs have been used to measure the horizontal components of the electric field fluctuations and three coils for the magnetic field variations. Magnetotelluric and magnetic transfer functions respectively impedance tensor and tipper, were extracted from time series of the five components. They were obtained over a period range extending from 0.001 s to 3,000 s (Fig. 4) using robust processing software provided by the instrument constructor that is based on Jones and Jödicke (1984), more exactly on method 6 in Jones et al. (1989).

DATA ANALYSIS

Magnetic transfer function analysis

The magnetic transfer function relates the vertical component to the two horizontal components of the magnetic field. It is theoretically zero for a one-dimensional Earth, and its value becomes non-null when there is a change in the lateral distribution of the electrical conductivity of the crust and upper mantle. It can be represented by the tipper that is equal to

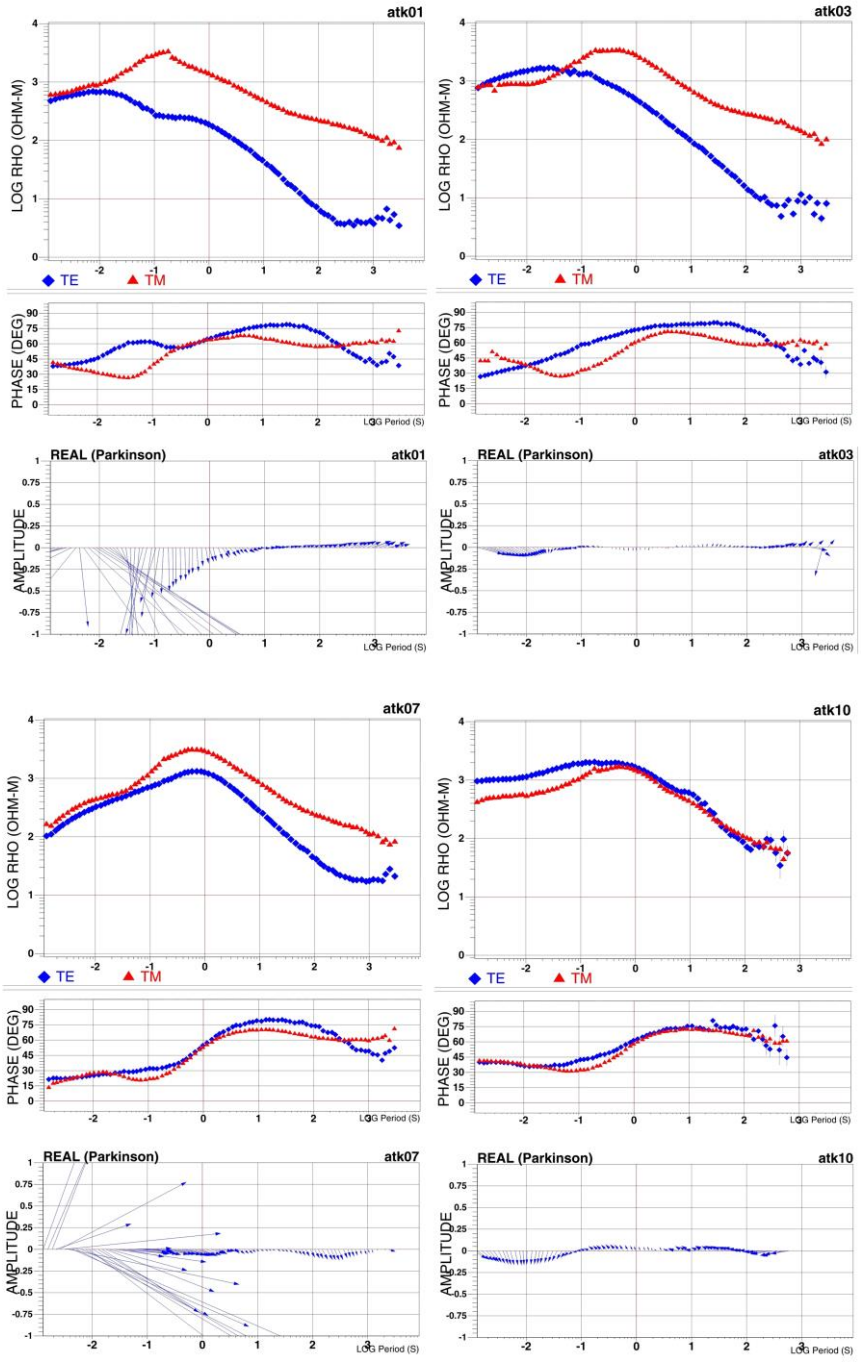

Fig. 4: TE (blue diamonds) and TM (red triangles) modes resistivity (top) and phase (center) data and induction vector real component (bottom) plotted following Parkison's (1962) convention of atk01, atk03, atk07 and atk10 magnetotelluric soundings.

the amplitude ratio of the vertical to the horizontal magnetic field components. In Hoggar, the tipper takes strong values at some sites. It is particularly strong for short periods

(<0.1 s) at atk01, atk02 and atk07, indicating the existence of shallow (<2 or 3 km) and local strong lateral contrasts in electrical conductivity. Reported on the geological map, these values appear to be likely due to the presence of faults (Figs. 1, 3). The tipper is moderately strong to weak for medium and short periods of all soundings, expressing the existence of more or less strong contrasts in electrical conductivity at a regional scale (Fig. 5).

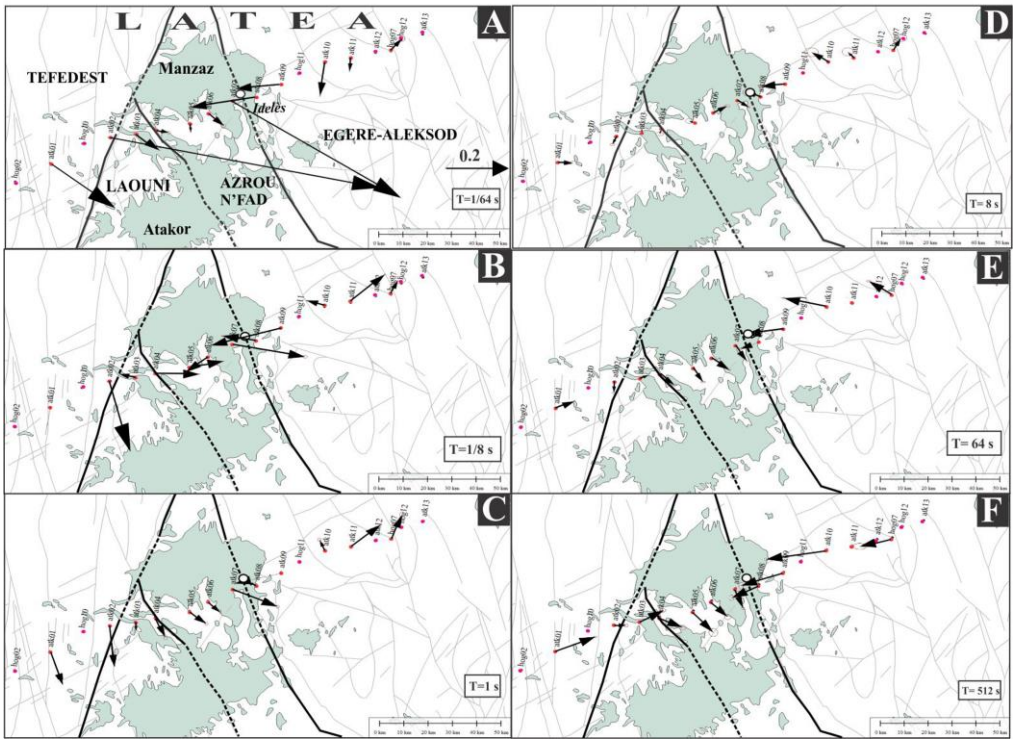

Fig. 5: Real component of the induction vectors plotted following Parkinson's (1962) convention corresponding to short and to long period data. Bad induction vectors are not shown on the figure.

Induction arrows or vectors are another way to represent the magnetic transfer function. The real induction vector drawn in Parkinson (1962) convention, is generally directed towards zones with high current concentrations that are more conductive areas (Jones, 1986). It has been plotted for all stations for the six periods corresponding to the shallow to deep penetration of the natural electromagnetic field (Fig. 5). The directions given by the induction vectors become more consistent from one site to another when going from short to long periods. For the longest periods (512 s, Fig. 5F), where the data are responding to the deep and regional structure, induction vectors are directed towards WSW to SW at sites located in the Egéré-Aleksod terrane, towards SSE to SE in the Azrou n'Fad terrane and finally towards NE to E in the Tefedest and Laouni terranes. These directions are fairly consistent with the regional geological trends shown up by various faults, especially the terrane boundaries that are of NW-SE to NNW-SSE direction. MT sites located in the center of the profile in the Azrou n'Fad terrane appear to be more affected by a large off-line conductive structure located to the south (Fig. 5).

Magnetotelluric impedance tensor analysis

To determine the geometry (or dimensionality) of the LATEA lithosphere beneath the magnetotelluric profile, we routinely performed the analysis of the impedance tensor of each of the 18 MT soundings following the method of Bahr (1988, 1991). The skew of Bahr (1988), which reflects the deviation from a 1-D or 2-D geometry, remains below the empirical threshold of 0.3 for most of the soundings. Instead, the skew of Swift (1967), which, in the absence of galvanic distortion of the data, gives the same information but is sensitive to the presence of superficial inhomogeneities of small size relative to the MT resolution, exceeds generally the threshold value of 0.06 (Marti et al., 2005; Fig. 6). The analysis of the impedance tensor of all MT soundings shows that, from the electrical point of view, the lithosphere under the MT profile can be best described by a 3-D/2-D model, i.e., a two-dimensional regional structure with superimposed small superficial three-dimensional inhomogeneities.

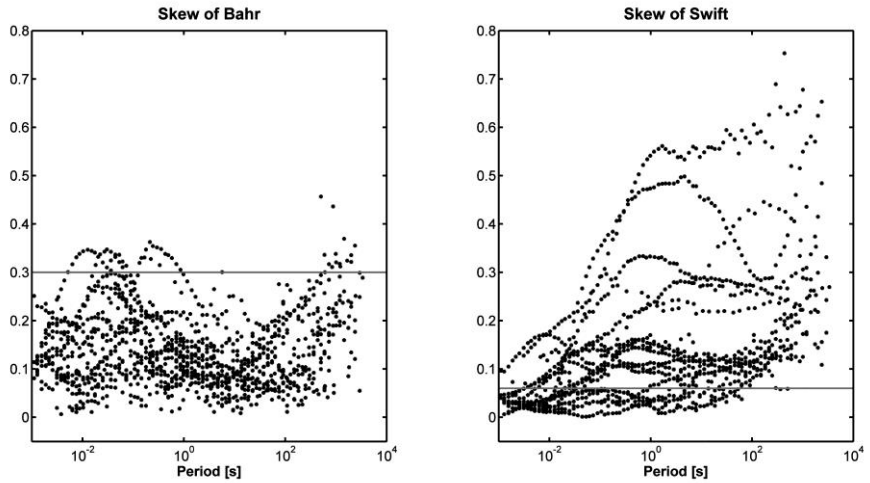

Fig. 6: Bahr's (left panel) and Swift's (right panel) skews of the entire MT soundings.

However, it is necessary to determine the azimuth of elongation of the regional structure also called the strike. The strike angle was calculated frequency by frequency for each sounding following the methods of Swift (1967), Bahr (1991) and Groom and Bailey (1989). Rose diagrams of the calculated strike angle are shown for four period ranges (Fig. 7): first, for all periods (Fig. 7, a, e, and I panels), then for short periods (<0.1 s) corresponding to the subsurface structure (Fig. 7, b, f, and j panels), for medium periods reflecting the effect of the upper and middle crust structure (Fig. 7, c, g and k panels), and last for long periods (> 10 s) corresponding to the deep crust and upper mantle structure (Fig. 7, d, h and l panels). The strike values calculated by Swift (1967) method may be affected by the galvanic distortion because this approach uses the impedance magnitude (Fig. 7, a, b, c and d panels). This is not the case for the Bahr (1991) method since it uses the phase of the impedance (Fig. 7, e, f, g and h panels). Groom and Bailey (1989) method

allows to estimate the strike by the least-squares fit of the data by a 3-D/2-D model (Fig. 7, I, j, k and l panels). Moreover, the estimation of the strike angle is quite difficult because it is very sensitive to the presence of noise in the data (Jones and Groom, 1993; McNeice and

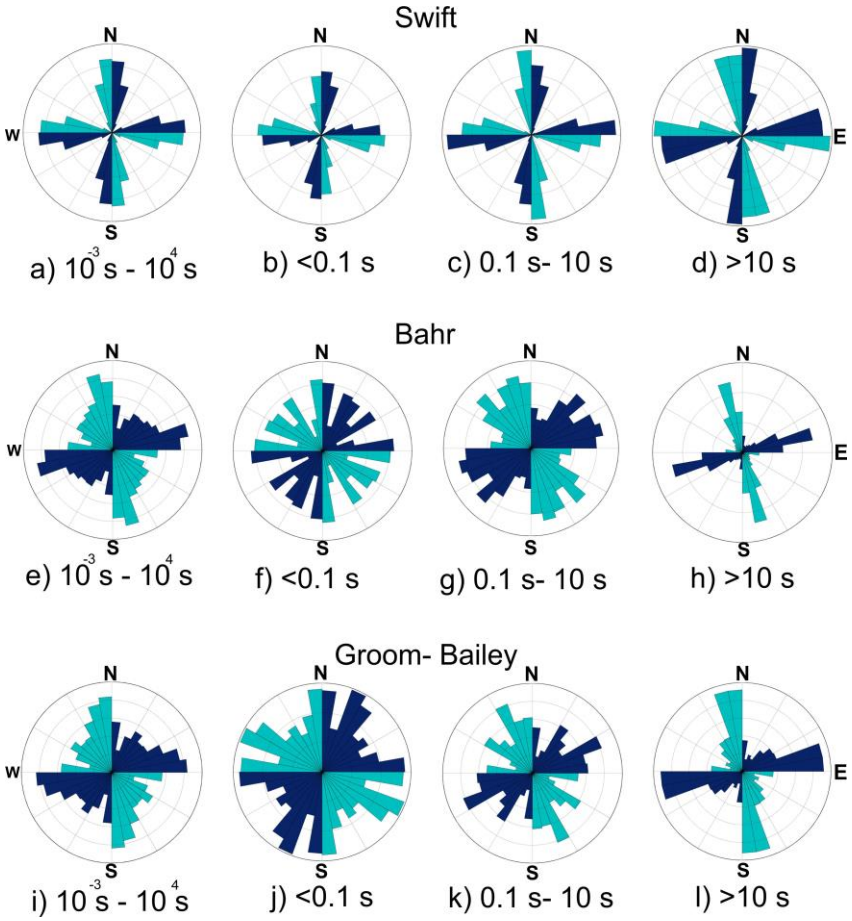

Fig. 7: Rose diagrams of strike angles determined by Swift (1967), Bahr (1991) and Groom and Bailey (1989) methods for different period ranges.

Jones, 2001). As our interest goes for the deep geological structure, we considered the strike angles calculated for the medium and long period data. Thus, we selected a strike at N15°W with however an ambiguity of 90° inherent to MT data. This uncertainty, however, is removed because the N15°W strike is consistent with the directions given by the induction vectors and the geological trends (Figs. 3, 5). At long periods, induction vectors point towards NE at stations located on Tefedest and Laouni terranes or SW part of the MT profile, and towards SW at those situated on Egéré-Aleksod terrane or NE part of the profile, while being perpendicular to directions of faults and shear zones especially the terrane boundaries of Azrou n'Fad (Fig. 5F).

Modeling the magnetotelluric data

The deep structure beneath Atakor area as shown by magnetotelluric data, can be validly interpreted as two-dimensional striking N15°W. This direction is supported by the magnetic transfer function data (Fig. 5). It corresponds as a whole to the elongation of the

Azrou n'Fad terrane and to its boundaries with the Egéré-Aleksod terrane to the east, and with the Laouni terrane to the west (Figs. 1, 3). The strike was then set to N15°W for all MT stations. TE and TM modes impedances that are not affected by the distortion, were then obtained according to the impedance tensor decomposition method of Groom and Bailey (1989). Transverse electric (TE) mode has been associated with the XY component and transverse magnetic (TM) mode to the YX component, with X directed to N15°W and Y directed to N75°E.

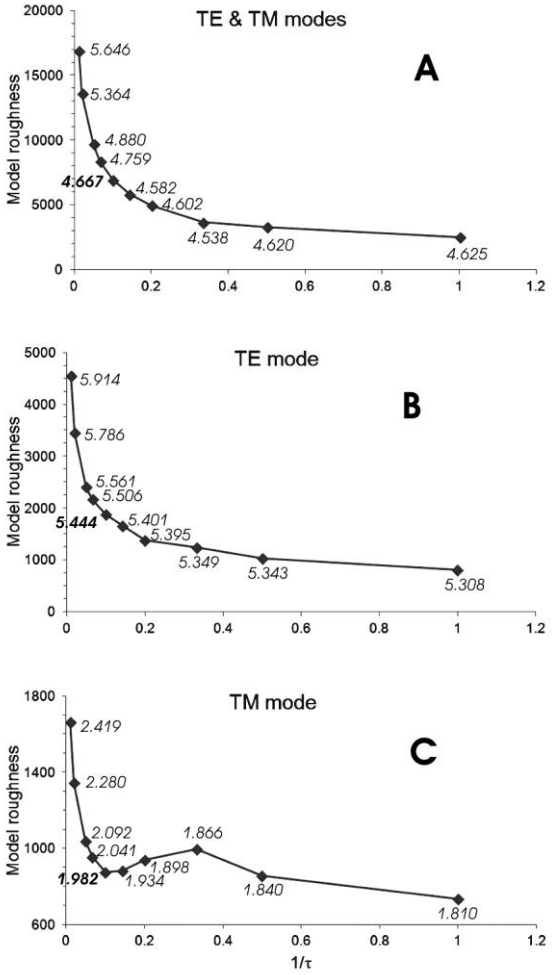

Fig. 8: The L-curve showing the model roughness versus the inverse of the regularization parameter τ for different rms obtained for TE and TM data (A), TE data only (B) and TM data only (C). The curve (in C) of the TM mode is more explicit. The "corner" corresponding to an rms of 1.982 and τ of 10 (1/τ= 0.1).

The depth of investigation in magnetotellurics is proportional to the square root of both the electrical resistivity of the geological formations and the period of electromagnetic waves. In the studied area, the Precambrian basement has very high electrical resistivity, exceeding several tens of thousands of Ω.m. On the other hand, each measurement site was occupied for about 20 hours, which allows obtaining MT impedance tensor responses to periods of the order of one hour, with good to high quality responses to around 1,000 s at most sites (see example data in Fig. 4). In the experimental conditions of this study, the depth of

investigation reaches thus more than one hundred km deep. In addition, greater penetration is generally obtained by the TM mode data that show much higher resistivity values at the longer periods (Fig. 4). The lateral resolution is <10 km, which is the average distance between the MT stations.

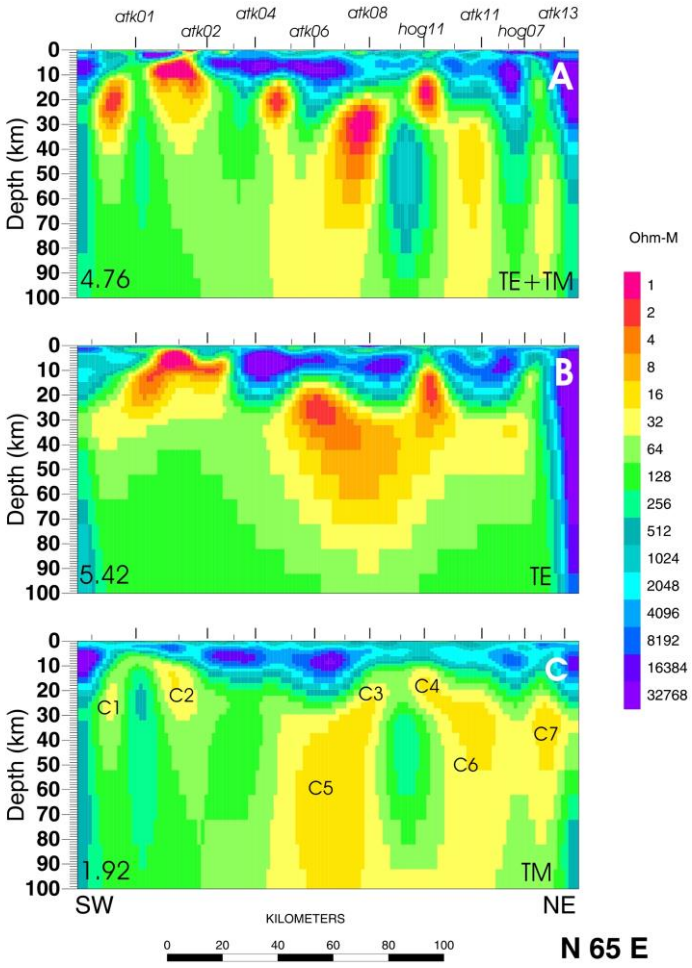

Fig.9: Two-dimensional models obtained by simultaneous inversion of apparent resistivity and phase data of both modes (with an rms of 4.76) in A, TE mode data only (rms of 5.42) in B, and TM mode data only (rms of 1.92) in C, using the NLCG algorithm of Mackie et al. (1997).

The magnetotelluric data were inverted using Mackie et al. (1997) two-dimensional (2-D) inversion algorithm that uses the finite difference method to calculate the forward responses of the various models found by the inversion process. The inversion algorithm is implemented within Geotools 7.30 software package. This algorithm version allows inverting the impedance tensor data but not tipper ones. With the exception of the regularization parameter τ and noise floor, all the other parameters are fixed and cannot be modified by the user. The mesh adopted in the electrical model has been sufficiently refined to reduce the value of the root mean square (rms) and better resolve changes in the conductivity distribution. The model responses were calculated for a subset of 19 available periods regularly distributed between 0.0038 s (260 Hz) and 1,000 s (0.001 Hz). As our interest is in

the deep structure, we did not invert the very short period data (<0.0038 s). To determine the optimum value of the regularization parameter τ, several tests were performed. Data of TE,

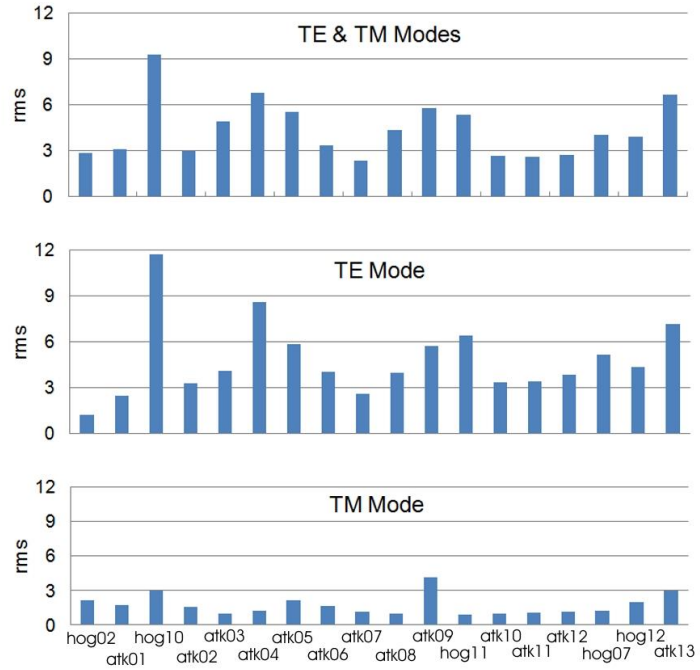

Fig. 10: Root mean square (rms) misfits along the MT profile for: data of the two modes (A, model of Fig. 9A), TE mode data only (B, model of Fig. 9B), and TM mode data only (C, model of Fig. 9C).

TM and both modes were inverted using starting models consist of a half-space of 10, 100 and 1,000 Ω.m, and for several values of τ (1 to 100). The error floor was fixed to 10% for apparent resistivity and 2.87° (equivalent to 5% on the impedance) for phase of both modes. The rms and model roughness values obtained in each case were used to build an L-curve (Hansen, 1992) for each mode separately and both as represented in Fig. 8. The L-curve of the TM mode shows more clearly that the optimum value of τ is equal to 10. This value was adopted for the calculation of all other electrical models shown in figure 9.

After various tests, we performed inversion of apparent resistivity and phase data of TE mode only, TM mode only and both modes. Each time, the starting model consists of a 100 Ω.m homogeneous and isotropic half-space. The regularization parameter was set to 10. The data of each mode separately, were inverted in two steps. First, the noise floor was set to 0.5 (50%) for the apparent resistivity and 2.87° (equivalent to 5% for impedance) for the phase. Then 0.1 and 2.87° respectively. The data of both modes are however inverted in four steps. (1) First, data of TM mode only with noise floor of 0.5 for the apparent resistivity and 2.87° for the phase. (2) Then, data of the TM mode only with noise floor of 0.1 and 2.87° respectively. (3) Data of both modes simultaneously with 0.1 and 2.87° for the TM mode apparent resistivity and phase respectively and 0.5 and 2.87° for the TE mode data. (4) Last, 0.1 and 2.87° for apparent resistivity and phase respectively of both modes.

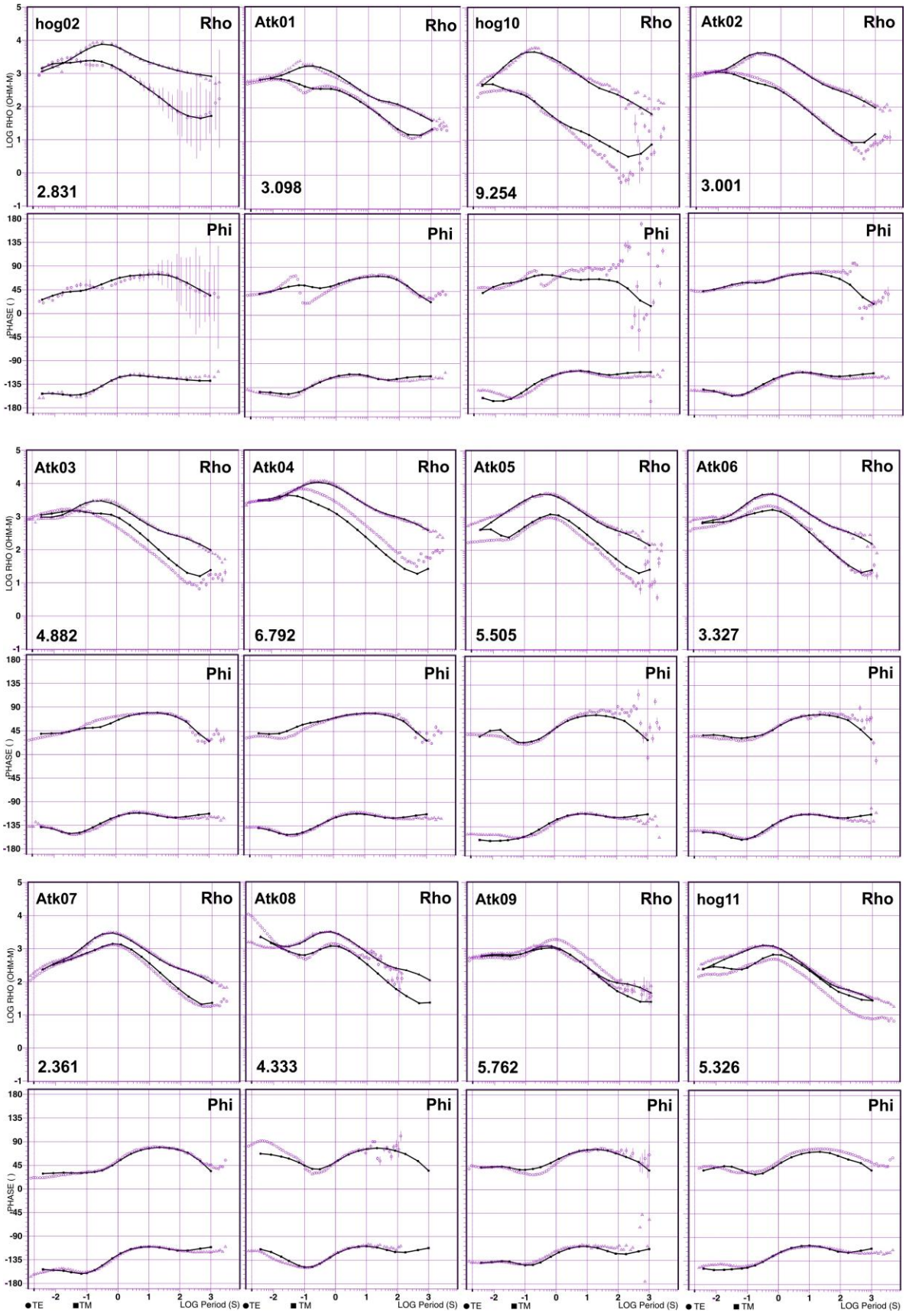

Fig. 11 (to be con't): TE (solid circle) and TM (solid square) modes resistivity and phase data fitted by the corresponding MT forward responses (curves) of the 2-D electric model shown in Fig. 9A.

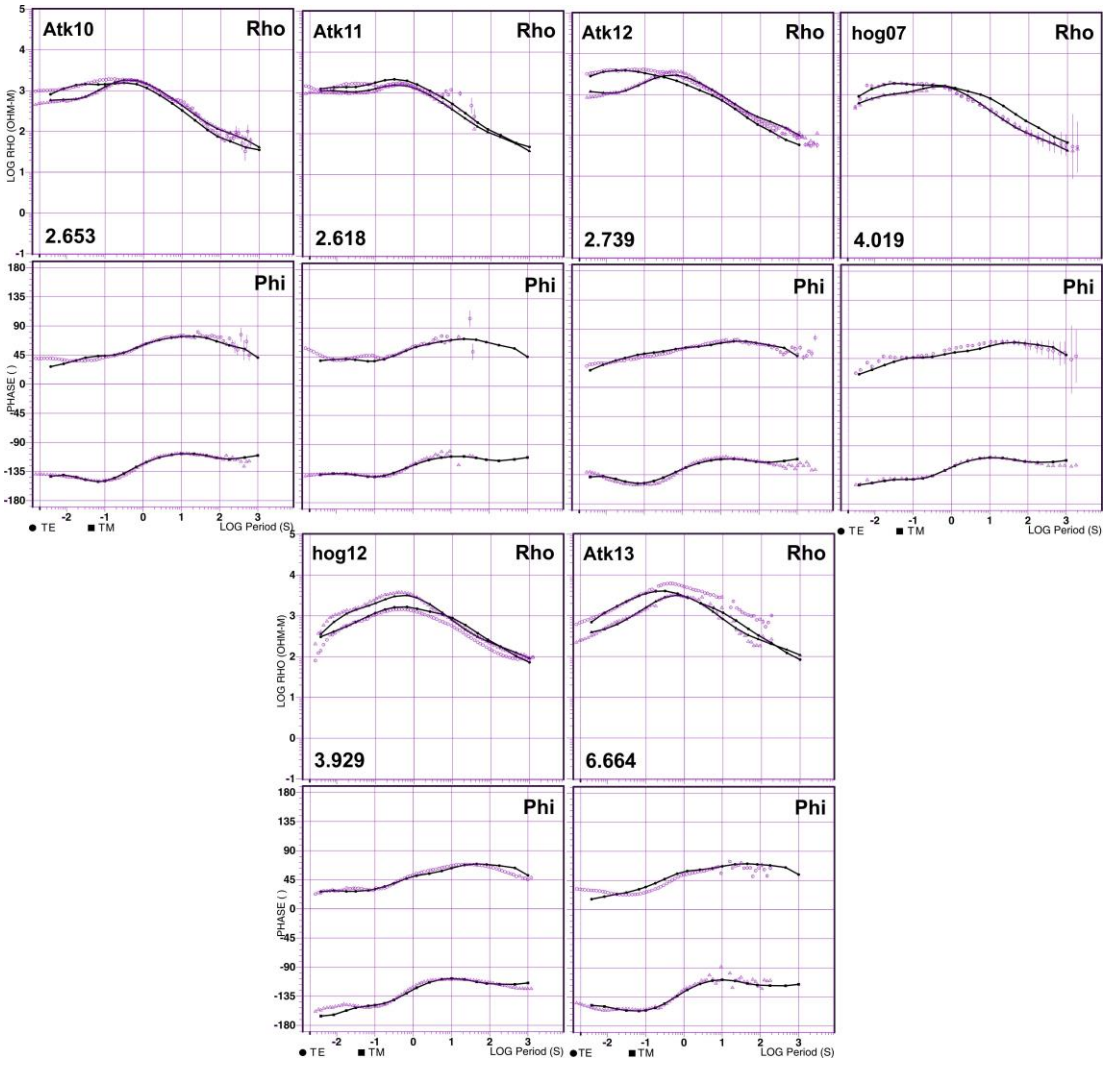

Fig. 11 (con't)

Figure 9 shows from top to bottom, models obtained by simultaneous inversion of data of both modes with an rms of 4.76 (in A), TE mode data (rms = 5.42, in B), and TM mode data (rms = 1.92, in C). The rms remain relatively high except that of the TM mode. The rms obtained for each station are however quite acceptable for this mode (Fig. 10C).

Data from some MT stations seem to be affected by a strong current channeling probably due to the presence of strong conductor corridors associated to the numerous faults that can be seen on the geological map. The current channeling effect is evident on some stations, particularly hog10 and atk08 (Fig.11). It is reflected on the TE mode by a sharp fall in the apparent resistivity and strong phase values at short periods (0.1 to 1 s on hog10) and very low values of apparent resistivity and phase dispersion at long periods (> 100 s for hog10). This is caused by strong attenuation of the electric field along the N15°W direction. In contrast, the TM mode data are much less affected by the current channeling but they are at the same time, less sensitive to the presence of thin subvertical conductors that are oriented in the NNW direction. Therefore, the electric model obtained by the inversion of TM

mode data (Fig. 9C) should reflect the roughly lithospheric structure of LATEA. Thin structures elongated in the strike direction will be difficult to be highlighted.

GEOLOGICAL INTERPRETATION AND DISCUSSION

The electric model obtained from magnetotelluric data reveals in Central Hoggar a resistive to very resistive upper crust typical of a Precambrian cratonic crust of generally > 10,000 Ω.m resistivity, 10 to 20 km thick and resting on a conductive lower crust of 100-500 Ω.m. The whole crust is underlain by a lithospheric mantle of 50 to 200 Ω.m resistivity. The presence of several conductors in the crust causes an attenuation of the electromagnetic energy and makes difficult the detection of any electrical signature associated with the Moho (Jones and Ferguson, 2001; Jones, 2013). Therefore, the MT data obtained here were not able to constrain the crustal thickness beneath the Atakor area in the same way as for the Archean terrane of In Ouzzal where, nevertheless, it was estimated from a one-dimensional modeling (Bouzid et al., 2008; Fig. 12).

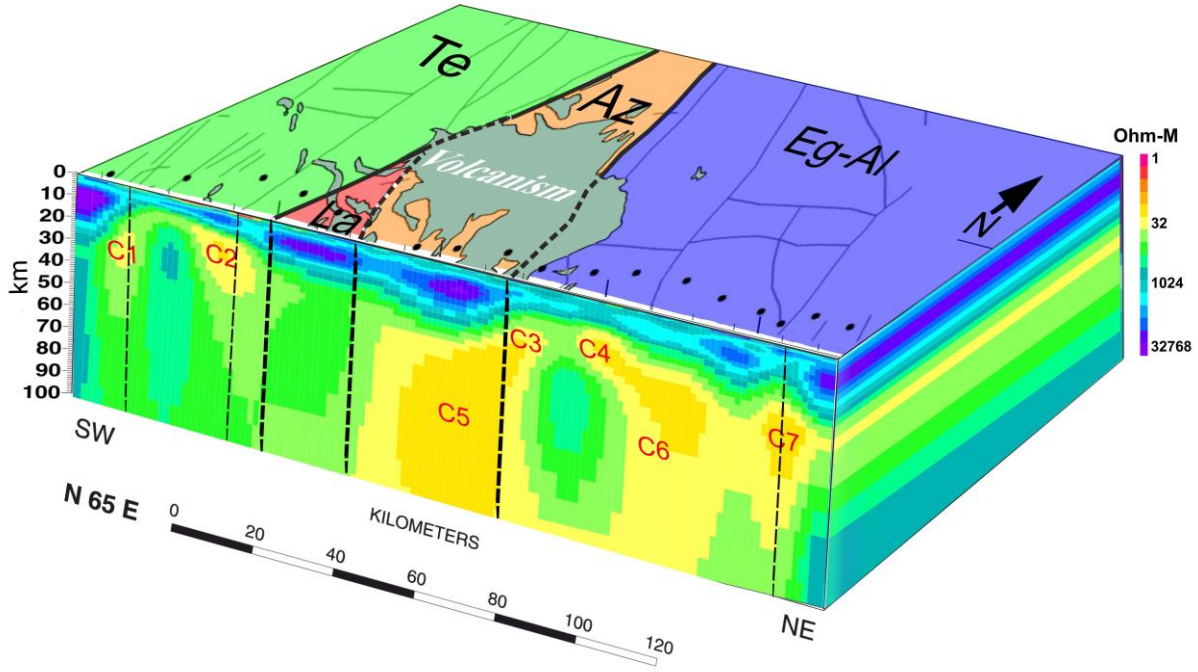

Fig. 12: 2-D electric model obtained by inversion of TM data of the entire MT profile stations (shown in Fig. 9C) with on the top the main geologic units of Central Hoggar. Te= Tefedest terrane, Az= Azrou n'Frad terrane, La= Laouni terrane, Eg-Al= Egéré-Aleksod terrane, and *volcanism* represents the Atakor/Manzaz Cenozoic volcanic districts (see Figs. 1, 3). The heavy dashed vertical lines represent the depth extension of the terrane boundaries delineated from the surface geology. The thin dashed vertical lines represent the depth extension of some intra-terrane faults corresponding to conductivity anomalies.

More importantly, the resistivity model shows that the Central Hoggar lithosphere is characterized by several subvertical more or less thin conductive structures of NNW-SSE elongation (C1 to C7). Some of these anomalies are crustal (C1 to C4) while others are rooted in the lithospheric mantle (C5, C6 and C7). Most of shallow conductivity anomalies

can be correlated with the various faults or shear zones identified on surface geology (Figs. 1, 3, 12). The C1 anomaly located directly below hog02 and atk01 stations and the C2, beneath hog10 and atk02 stations (Figs. 3, 8, 12), are associated to numerous faults affecting the In Amguel area. The geological map (Fig. 3) shows that this area is affected by several faults trending NS to NNW-SSE and to a lesser degree NE-SW thus subdividing the crust into several blocks. According to Liu and Gao (2010), the Tefedest terrane has a well-developed fault system reflecting a mechanically rather brittle crust. The C3 anomaly is located at the lower crust beneath atk08 and coincides with the terrane boundary separating Azrou n'Fad from Egéré-Aleksod. C4, located beneath hog11, does not match any known fault.

The deep C5 anomaly is located under atk04 to atk08 stations directly below Atakor/Manzaz volcanic massifs whose last activity is as recent as the Holocene (Liégeois et al., 2005; Azzouni-Sekkal et al., 2007). The top of this anomaly is located at the base of the crust and its lateral edges correspond remarkably to both inter-terrane shear zones limiting Azrou n'Fad with Laouni, to the west, and with Egéré-Aleksod, to the east. Although, because of the loss of resolution of the method with depth, the anomaly could be thinner and more conductive. The increase in conductivity may be caused by the presence of trapped fluids, partial melts or mineralization at shear zones during the rise of the magma to the surface. The C6 anomaly located below hog11 to atk11 stations, although clearly highlighted by the resistivity model, does not seem to be correlated with a known fault. The resistivity model shows that this anomaly is however connected to C4. Located near the NE end of the profile below hog12, C7 fits well a NNW-SSE fault. So, even if the correspondence between the resistivity model and the mapped major faults is not perfect, even if good, the resistivity model reveals a structure very close to that which is mapped. In addition, the resistivity model brings constraints on the deep geometry of these fault and on the thickness on which they are active.

The heat flow and P-wave seismic tomography data do not show any regional anomaly across the Hoggar but reveal the existence of more localized lithospheric anomalies associated with Atakor volcanic district (Lesquer et al., 1988, Lesquer et al., 1989; Ayadi et al., 2000). Likewise, the MT data show localized electrical anomalies that can be associated to the Pan-African structure of the Hoggar as well as to the Cenozoic volcanism of Atakor/Manzaz districts. The resistivity model suggests a rise of magma/fluid along the lithospheric mega-shear zones under Atakor, especially along the inter-terrane shear zones limiting the Azrou N'Fad terrane. Possible spreading of magma beneath the Moho discontinuity would have released fluids in the lower crust, a phenomenon able to increase its conductivity as it is the case beneath the Tefedest and Egéré-Aleksod terranes (Fig. 12). When moving upward, these magmas and fluids can be trapped in faults and shear zones,

which is also imaged by the magnetotellurics. Magma upwelling with fluid release is also highlighted through magnetotelluric data beneath the Great Basin-Colorado Plateau transition zone in Utah (Wannamaker et al., 2008; Meqbel et al., 2014).

The generation and rise of magmas can promote vertical delamination and removal of lithospheric mantle (Liégeois et al., 2003; 2013). In some peculiar case, such as below the major Atakor and Manzaz district, this lithospheric removal can be larger, as proposed by Beccaluva et al. (2007, their figure 9) allowing a more important asthenosphere uprise. This can explain the different lower crust electric signature of the Azrou n'Fad terrane above which are located the Atakor and Manzaz volcanic districts. This is in agreement, on a small scale, with the results of receiver function data analysis in the Tamanrasset region in the southwest end of the Atakor (Liu and Gao, 2010). However, let is stress that the isotopic signature of the Hoggar volcanism point to a depleted mantle signature (e.g. Dautria et al., 1988; Beccaluva et al., 2007) without hybridization, even in small amount, with the old Precambrian crust, which has a contrasted strongly enriched signature. Ponding of large amounts of magmas within the crust is thus precluded.

The electrical model constraints allow discussing the various hypotheses proposed by several authors, related to the Hoggar lithospheric structure, the source of the Cenozoic volcanism and the origin of the specific morphology of the Hoggar swell. According to Lesquer et al. (1988), the Hoggar is characterized by a strong negative gravity anomaly and a normal heat flow (Fig. 2). These observations have been interpreted as being due to the introduction before the Eocene (i.e. before 60 Ma) of an ENE-WSW elongated light body, with lateral dimensions of 200 km x 400 km, located under the base of the crust at a depth of 50 km. However, according to the authors, the gravity data do not exclude the possibility that the light body extends to the whole lithospheric mantle. Taking into account the absence of heat flow anomaly as a dissipated thermal anomaly, Lesquer et al. (1988) considered that this light body represents cooled metasomatized lithospheric mantle. This assumption allows explaining both the Hoggar morphology and the Anahef tholeiitic volcanism, regarded as the most important volcanic district in volume of the Hoggar. Moreover, for Aït-Hamou and Dautria (1994) and Aït-Hamou et al. (2000), the Hoggar swell and the Cenozoic volcanism are due to the thermal effect produced by the presence, since the Eocene, of a mantle plume beneath Hoggar. The plume would have caused a lightening of the upper lithospheric mantle up to a hundred km depth and even 80 km under the Atakor volcanic district (Aït-Hamou and Dautria, 1994 and references therein). However, the existence of lightened and highly modified lithospheric mantle by reheating, partial melting, recristallization, metasomatism and magmatic veining of Late Mesozoic to Early Cenozoic (Lesquer et al., 1988), even if completely cooled now, would imply a significant increase in electrical conductivity at the regional scale. This is not shown by the magnetotelluric data which do not reveal any

conductivity anomaly beneath the study area at such a scale. In consequence, MT data do not support these hypotheses except if the metasomatized upper mantle area is located deeper, beyond the depth of investigation of our MT data, i.e. >100 km.

The Hoggar swell has also been explained by a lithospheric thinning produced by the thermal effect of an asthenospheric upwelling that began from the Lower Eocene (Beccaluva et al., 2007; Rougier, 2012). From a two-dimensional modeling of free air gravity, geoid and topographic data, Rougier (2012) estimated the thickness of the lithosphere beneath Atakor to about 55 km with the assumption, however, of a thin crust (34 km). The rise of the lithosphere/asthenosphere boundary (LAB) up to 55 km would imply a significant fall beneath the entire study area, of the resistivity to about 10 Ω.m which is the signature of the electrical asthenosphere (Jones, 1999 and references therein). Instead, the electrical model shows much larger values of about 100 Ω.m, typical resistivity of the continental lithospheric mantle (Haak, 1980; Lastoviskova, 1983; Jones, 1999). Moreover, the C5 deep anomaly revealed by the MT data is subvertical and of less than a few tens of km thickness, which is too thin to correspond to an asthenospheric rise due to lithospheric thinning under the Atakor area. MT data do not favor such a model either. Again, a thinning located at a depth >100 km in a thick lithosphere could not be seen by our MT data, but this case was considered as not likely by Beccaluva et al. (2007) and Rougier (2012).

For Liégeois et al. (2005) as well as for Azzouni-Sekkal et al. (2007), the Cenozoic volcanism that accompanied the rising of Hoggar Swell, was produced by passive adiabatic ascent of melts from the lithosphere/asthenosphere boundary at 160 km deep along mega-shear zones due to their reactivation in response to the remote collision of African and Eurasian plates. According to these authors, the absence of a heat flow anomaly in the Hoggar is inconsistent with the hypothesis of a regional lithospheric thinning by thermal effect but could be reconciled with linear (planar) thinning along shear-zones. The value of 63 mW/m^2 observed south of Atakor was interpreted as a local effect of Atakor volcanism (Lesquer et al, 1989; Liégeois et al, 2005). This led Liégeois et al. (2005) to suggest placing the source of the negative gravity anomaly observed in Central Hoggar at greater depth, at least 250 km, well below the one proposed by Lesquer et al. (1988). Indeed, the reactivation of mega-shear zones does not imply a large scale conductivity anomaly but thin subvertical anomalies along the different shear zones due to linear delamination (Liégeois et al., 2003; 2013). The electrical signature of such structures could only be detected by high-resolution MT data, as those acquired during this study: the electrical model deduced from the magnetotelluric data of this study shows no regional anomaly under Atakor area, but reveals a set of subvertical more or less thin conductors, in agreement with an intraplate metacratonic process induced by the distant stress provoked at plate margin by the Europe-Africa collision (Liégeois et al., 2005; 2013). This implies that the Hoggar Cenozoic

volcanism is triggered by the lithosphere response to stress at the plate margin, allowing mantle melts coming from the fertile lower lithosphere or lithosphere-asthenosphere boundary (perisphere; Anderson & Sammis, 1970; Anderson, 1994; Black & Liégeois, 1993) and does not have deep mantle causes, such as mantle plumes (Anderson, 2001). The rheological structure of metacraton is also essential: rigid but broken by lithospheric-scale shear zones, metacratonic areas are prone to be reactivated in intraplate settings (Liégeois et al., 2013). The models generated from the magnetotelluric data here reported demonstrate that lithospheric metacratonic shear zones correspond now to fluid pathways and are thus active, explaining the localization of the Hoggar swell and volcanism.

CONCLUSIONS

For modeling the deep electrical structure of the Hoggar down to a depth of c. 100 km, magnetotelluric (MT) data were collected at 18 sites along a 170 km-long profile. The MT profile spreads over the four LATEA metacratonic terranes (Central Hoggar) and crosses the area of the Atakor and Manzaz volcanic districts, covering the central part of the Hoggar swell. The electrical model obtained shows a resistive upper crust above a conductive lower crust, the whole resting on an even more conductive lithospheric mantle. This electrically common lithospheric structure is interestingly marked by subvertical conductors, some being of crustal scale while others are of lithospheric scale. Most of these conductors can be associated with shear zones known at the surface.

More precisely, the features in the MT model are correlated with fluids circulating along these shear zones, meaning that the latter are still active today and have thus probably functioned vertically during the Cenozoic uplift leading to the current Hoggar swell. Our MT data provide thus further arguments to constrain the controversial process currently at work under this swell. They do not show any conductivity anomaly of regional size required (1) for a recent metasomatism of the lithosphere as proposed by Lesquer et al. (1988), (2) for a mantle plume head below Hoggar (Ait Hamou et al., 2000), (3) for a lithospheric thinning bringing the lithosphere/asthenosphere boundary up to a depth of 55 km (Rougier, 2012). Our MT data are not fully consistent with these hypothesis as well as with all models claiming for a large thermal anomaly at a depth <100 km below Hoggar and is in favor of a top-down tectonics (Anderson, 2001), i.e. that these processes are generated within the lithosphere by distant lithospheric stress and not by deep lower mantle processes.

On the other hand, the present MT data agree with the metacratonic model for LATEA (Liégeois et al., 2003; 2005; 2013), which introduces planar delamination along pre-existing shear zones allowing the rising of magmas and relative vertical movements between the terranes constituting LATEA, without a global thinning of the lithosphere. At the present time, in opposition to the Pan-African times, this intraplate reactivation due to far-field stress

(Africa-Europe convergence) produced limited amounts of magmatism and only vertical movements (generating the swell) but imply the passage of volcanic melts and fluids along the shear zones. This is in agreement with the electrical model implying the absence of a large thermal anomaly at depth but fluids along shear zones. No influence of deep phenomena such as mantle plumes are observed and they are not needed. In turn, our MT data provide further new evidence for the volcanic-generating metacratonic process, until now only deduced from indirect observations.

ACKNOWLEDGMENTS

This study was conducted in the framework of the Algerian/French Tassili cooperation program n° 12MDU878: “Evolution géodynamique méso-cénozoïque des régions de l’Atakor et du Serouanout”. We thank M. Derder and Y. Missenard for the many fruitful discussions that we had together. The field campaign was carried out with the support of CRAAG. We thank the civil and military authorities of the Wilaya of Tamanrasset for their assistance in achieving the field campaign. We are indebted to Don Anderson both for his pioneering works having shown that the cause of the intraplate magmatism must be searched in the lithosphere and not in the lower mantle and for his continued efforts for stressing the need for not violating the physical laws when modeling the behavior of the Earth mantle. This paper was reviewed by B. Bonin, Ph. Wannamaker and an anonymous reviewer who by their criticism led to a substantial improvement of its content. They are warmly thanked by the authors. We also thank Gillian Foulger for her fast and efficient editorial handling. Finally, we would like to acknowledge Don Anderson for always prioritizing fact over fantasy, whilst at the same time erecting innovative models with far-reaching consequences.

REFERENCES CITED

Abdallah, N., Liégeois, J.-P., De Waele, B., Fezaa, N., and Ouabadi, A., 2007, The Temaguessine Fe-cordierite orbicular granite (Central Hoggar, Algeria): U–Pb SHRIMP age, petrology, origin and geodynamical consequences for the late Pan-African magmatism of the Tuareg shield: Journal of African Earth Sciences, v. 49, p. 153-178.

Abdelsalam, M., Liégeois, J. P., and Stern, R. J., 2002, The Saharan metacraton: Journal of African Earth Sciences, v. 34, p. 119-136.

Acef, K., Liégeois, J.P., Ouabadi, A., and Latouche, L., 2003, The Anfeg post-collisional Pan-African high-K calc-alkaline batholith (Central Hoggar, Algeria), result of the Latea microcontinent metacratonisation: Journal of African Earth Sciences, v. 37, p. 295–311.

Adjerid, Z., Ouzegane, K., Godard, G., and Kienast, J.-R. 2008, First report of ultrahigh- temperature sapphirine spinel quartz and orthopyroxene+ spinel+ quartz parageneses discovered in Al–Mg granulites from the Khanfous area (In Ouzzal metacraton, Hoggar, Algeria), In Ennih, N. and Liégeois, J.-P., eds, The Boundaries of the West African Craton: Geological Society, London, Special Publications, v. 297, p. 147–167.

Aït-Hamou, F., and Dautria, J.M., 1994, Le magmatisme cénozoïque du Hoggar: une synthèse des données disponibles. Mise au point sur l'hypothèse d'un point chaud: Bulletin du Service Géologique de l'Algérie, v. 5, p. 49-68.

Aït-Hamou, F., Dautria, J.M., Cantagrel, J.M., Dostal, J., and Briqueu, L., 2000, Nouvelles données géochronologiques et isotopiques sur le volcanisme cénozoïque de l'Ahaggar (Sahara algérien): Des arguments en faveur d'un panache: Comptes Rendus de l'Académie des Sciences de Paris, v. 330, p. 829–836.

Anderson, D.L., 1994, The sublithospheric mantle as the source of continental flood basalts; the case against the continental lithosphere and plume head reservoirs: Earth and Planetary Science Letters, v. 123, p. 269–280.

Anderson, D.L., 2001, Top-Down Tectonics? : Science, v. 293, p. 2016-2018.

Anderson, D.L., and Sammis, C., 1970, Partial melting in the upper mantle: Physics of the Earth and Planetary Interiors, v. 3, p. 41-50.

Ayadi, A., Dorbath, C., Lesquer, A., and Bezzeghoud, M., 2000, Crustal and upper mantle velocity structure of the Hoggar swell (central Sahara, Algeria): Physics of the Earth and Planetary Interiors, v. 118, p. 111–123.

Azzouni-Sekkal, A., Bonin, B., Benhallou, A. Yahiaoui, R., and Liégeois, J.P., 2007, Cenozoic alkaline volcanism of the Atakor massif, Hoggar, Algeria, in Beccaluva, L., Bianchini, G. and Wilson, M., eds., Cenozoic Volcanism in the Mediterranean Area, Special Publication, Geological Society of America, v. 418, p. 321–340.

Bahr K., 1988, Interpretation of the Magnetotelluric Impedance Tensor: Regional Induction and Local Telluric Distortion: Journal of Geophysics, v. 62, p. 119-127

Bahr, K., 1991, Geological noise in magnetotelluric data: a classification of distortion types: Physics of the Earth and Planetary Interiors, v. 66, p. 24-38.

Beccaluva, L., Azzouni-Sekkal, A., Benhallou, A., Bianchini, G., Ellam, R.M., Marzola, M., Siena, F., and Stuart, F.M., 2007, Intracratonic asthenosphere upwelling and lithosphere rejuvenation beneath the Hoggar swell (Algeria): Evidence from HIMU metasomatised lherzolite mantle xenoliths: Earth and Planetary Science Letters, v. 260, p. 482–494.

Bendaoud, A., Ouzegane, K., Godard, G., Liégeois, J.P., Kienast, J.R., Bruguier, O., and Drareni, A., 2008, Geochronology and metamorphic P–T–X evolution of the Eburnean granulite-facies metapelites of Tidjenouine (Central Hoggar, Algeria): witness of the LATEA metacratonic evolution, *in* Ennih, N., and Liégeois, J.-P., eds., The Boundaries of the West African Craton, Geological Society, London, Special Publication 297, p. 111–146.

Bertrand, J.M., and Caby, R., SONAREM, compilers, 1977, Carte géologique du Hoggar, Sonarem, scale 1:1,000,000, 2 sheets.

Black R., and Liégeois J.P., 1993, Cratons, mobile belts, alkaline rocks and continental lithospheric mantle: the Pan-African testimony: Journal of the Geological Society of London, v. 150, p. 89-98

Black, R., Latouche, L., Liégeois, J.P., Caby, R., and Bertrand, J.M., 1994, Pan-African displaced terranes in the Tuareg shield (central Sahara): Geology, v. 22, p. 641–644.

Bouzid, A., Abtout, A., and Akacem, N., 2004, Electrical structure of the crust and upper mantle of the Hoggar shield from magnetotelluric data: Colloquium of African Geology, 20th, Orléans, France, Abstracts, 438 p.

Bouzid, A., Akacem, N., Hamoudi, M., Ouzegane, K., Abtout, A., and Kienast, J.-R., 2008, Modélisation magnétotellurique de la structure géologique profonde de l'unité granulitique de l'In Ouzzal (Hoggar

occidental): Comptes Rendus Geoscience, v. 340, p. 711-722 (in French with an abridged English version).

Cagniard, L., 1953, Principe de la méthode magnétotellurique, nouvelle méthode de prospection géophysique: Annales de Géophysique, v. 9, p. 95-125.

Crough, S.T., 1981, Free-air gravity over the Hoggar massif, northwest Africa: Evidence for the alteration of the lithosphere: Tectonophysics, v. 77, p. 189–202.

Dautria, J. M., Dostal, J., Dupuy, C., and Liotard, J. M., 1988, Geochemistry and petrogenesis of alkali basalts from Tahalra (Hoggar, Northwest Africa): Chemical Geology, v. 69, p. 17-35.

Fezaa, N., Liégeois, J.P., Abdallah, N., Cherfouh, E.H., De Waele, B., Bruguier, O., and Ouabadi, A., 2010, Late Ediacaran geological evolution (575–555 Ma) of the Djanet Terrane, Eastern Hoggar, Algeria, evidence for a Murzukian intracontinental episode: Precambrian Research, v. 180, p. 299–327.

Fishwick, S., and Bastow, I.D., 2011, Towards a better understanding of African topography: a crust and upper mantle review of passive-source seismic studies of the African crust and upper mantle: Geological Society, London, Special Publications 357, p. 343–371.

Gangopadhyay, A., Pulliam, J., and Sen, M.-K., 2007, Waveform modeling of teleseismic S, Sp, SsPm P, and shear-coupled PL waves for crust-an d upper-mantle velocity structure beneath Africa: Geophysical Journal International, 170, 1210-1226.

Groom, R. W., and Bailey, R. C., 1989, Decomposition of magnetotelluric impedance tensor in the presence of local three-dimensional galvanic distortion: Journal of Geophysical Research, v. 94, p. 1913-1925.

Haak, V., 1980, Relations between electrical conductivity and petrological parameters of the crust and upper mantle: Geophysical Surveys, v. 4, p. 57-69.

Hansen, C., 1992, Analysis of discrete ill-posed problems by means of the L-curve: SIAM Review, 34, 4, 561-580.

Harinarayana, T., Patro, B. P. K., Veeraswamy, K., Manoj, C., Naganjaneyulu, K., Murthy, D. N., and Virupakshi, G., 2007, Regional geoelectric structure beneath Volcanic Province of the Indian subcontinent using magnetotellurics: Tectonophysics, v. 445, p. 66-80.

Hazler, S. E., Sheehan, A. F., McNamara, D. E., and Walter, W. R. , 2001, One-dimensional shear velocity structure of Northern Africa from Rayleigh wave group velocity dispersion: Pure and Applied Geophysics, v. 158, p. 1475-1493.

Jödicke, H., 1992, Water and graphite in the earth's crust an approach to interpretation of conductivity models: Surveys in Geophysics, v. 13, p. 381-407.

Jones, A.G., 1986, Parkinson's pointers' potential perfidy!: Geophysical Journal of the Royal Astronomical Society, v. 87**,** p. 1215-1224.

Jones, A. G., 1993, The COPROD2 dataset - tectonic setting, recorded MT data, and comparison of models: Journal of Geomagnetism and Geoelectricity, v. 45, p. 933-955.

Jones, A. G., 1999, Imaging the continental upper mantle using electromagnetic methods: Lithos, v. 48, p. 57-80.

Jones, A. G., 2013, Imaging and observing the electrical Moho: Tectonophysics, v. 609, p. 423-436.

Jones, A. G., and Groom, R. W., 1993, Strike-angle determination from the magnetotelluric impedance tensor in the presence of noise and local distortion: rotate at your peril!: Geophys. J. Int., 113,524-534.

Jones, A. G., and Ferguson, I. J., 2001, The electric Moho: Nature, v. 409, p. 331-333.

Jones, A. G., and Jödicke, H., 1984, Magnetotelluric transfer function estimation improvement by a coherence-based rejection technique, *in* Proceedings, Annual International Society of Exploration Geophysists Meeting, 54th, Atlanta, Georgia 51-55.

Jones, A. G., Chave, A. D., Egbert, G. Auld, D., and Bahr, K., 1989, A comparison of techniques for magnetotelluric response function estimation: Journal of Geophysical Research, v. 94, p. 14201-14213.

Jones, A. G., Kurtz, R. D., Boerner, D. E., Craven, J., A., McNeice, G. W., Gough D. I., DeLaurier, J. M., and Ellis R. G., 1992, Electromagnetic constraints on strike-slip fault geometry – The Fraser River fault system: Geology, v. 20, p. 561-564.

Lastoviskova, M., 1983, Laboratory measurement of electrical properties of rocks and minerals: Geophysical Surveys, v. 6, p. 201-213.

Lesquer, A., Bourmatte, A., and Dautria, J. M., 1988, Deep structure of the Hoggar domal uplift (Central Sahara, South Algeria) from gravity, thermal and petrological data: Tectonophysics, v. 152, p. 71-87.

Lesquer, A., Bourmatte, A., Ly, S., and Dautria, J.M., 1989, First heat flow determination from the Central Sahara: Relationship with the Pan-African belt and Hoggar domal uplift: Journal of African Earth Sciences, v. 9, p. 41–48.

Liégeois J.P., Black R., Navez J. and Latouche L., 1994, Early and late Pan-African orogenies in the Aïr assembly of terranes (Tuareg shield, Niger): Precambrian Research, v. 67, p. 59-88.

Liégeois J.P., Navez J., Hertogen, J. and Black R., 1998, Contrasting origin of post-collisional high-K calc-alkaline and shoshonitic versus alkaline and peralkaline granitoids: Lithos, v. 45, p. 1-28.

Liégeois, J. P., Latouche, L., Boughrara, M., Navez, J., and Guiraud, M., 2003, The LATEA metacraton (Central Hoggar, Tuareg shield, Algeria) : behaviour of an old passive margin during the Pan-African orogeny: Journal of African Earth Sciences, v. 37, p. 161-190.

Liégeois, J.-P., Benhallou, A., Azzouni-Sekkal, A., Yahiaoui, R., and Bonin, B., 2005, The Hoggar swell and volcanism: Reactivation of the Precambrian Tuareg shield during Alpine convergence and West African Cenozoic volcanism: Geological Society of America Special Paper, v. 388, p. 379-400.

Liégeois, J.-P., Abdelsalam, M. G., Ennih, N., and Ouabadi, A., 2013, Metacraton: Nature, genesis and behavior: Gondwana Research, v. 23, p. 220-237

Liu, H. L., and Gao S. S., 2010, Spatial variations of crustal characteristics beneath the Hoggar swell, Algeria, revealed by systematic analyses of receiver functions from a single seismic station: Geochemistry Geophysics Geosystems, v. 11, article Q08011.

Mackie, R., Rieven S., and Rodi, W., 1997, Users manual and software documentation for two-dimensional inversion of magnetotelluric data, Software implemented in GEOTOOLS, Massachusetts Institute of Technology, 13 pp.

Marti, A., Queralt, P., Jones, A. G., and Ledo, J., 2005, Improving Bahr's invariant parameters using the WAL approach: Geophysical Journal International, v. 163, p. 38-41

Maza, M., Briqueu, L., Dautria, J.-M., and Bosch, D., 1998, The Achkal Oligocene ring complex Sr, Nd, Pb evidence for transition between tholeitic and alkali Cenozoic magmatism in central Hoggar (South Algeria): Comptes Rendus de l'Académie des Sciences de Paris,Série IIa, v. 327, p. 167–172.

McNeice, G.W. and A.G. Jones, 2001, Multisite, multifrequency tensor decomposition of magnetotelluric data: Geophysics, 66, 158-173.

Meert, J. G., and Lieberman, B. S., 2008, The Neoproterozoic assembly of Gondwana and its relationship to the Ediacaran–Cambrian radiation: Gondwana Research, v. 14, p. 5–21.

Meqbel, N. M., Egberta, G. D., Wannamaker, Ph. E., Kelberta, A. and Schultz, A., 2014, Deep electrical resistivity structure of the northwestern U.S. derived from 3-D inversion of USArray magnetotelluric data: Earth and Planetary Science Letters, v. 402, p. 290–304.

Merlet, J., 1962, Note relative aux phases sismiques observées entre 100 et 200 km dans le massif du Hoggar: Comptes rendus de l'Académie des Sciences, v. 255, p. 3441 - 3443.

Nover, G., 2005, Electrical proprieties of crustal and mantle rocks a review of laboratory measurements and their explanation: Surveys in Geophysics, v. 26, p. 593-651.

Parkinson, W. D., 1962, The influence of continents and oceans on geomagnetic variations: Geophysical Journal of the Royal Astronomical Society, v. 6, p. 441-449.

Pasyanos, M. E., and Walter, W. R., 2002, Crust and upper-mantle structure of North Africa , Europe and the Middle East from inversion of surface waves: Geophysical Journal International, v. 149, p. 463-481.

Peucat, J.J., Drareni, A., Latouche, L., Deloule, E., and Vidal, P., 2003, U–Pb zircon (TIMS and SIMS) and Sm-Nd whole rock geochronology of the Gour Oumalelen granulitic basement, Hoggar massif, Tuareg Shield, Algeria: Journal of African Earth Science, v. 37, p. 229–239.

Ritter, O., Weckmann, U., Vietor, T., and Haak, V., 2003, A magnetotelluric study of the Damara Belt in Namibia. 1. Regional scale conductivity anomalies: Physics of the Earth and Planetary Interiors, v. 138, p. 71-90.

Roberts, G. G., and White, N., 2010, Estimating uplift rate histories from river profiles using African examples: Journal of Geophysical Research, v. 115, B02406, 1-24.

Rossi, P.L., Lucchini, F., and Savelli, C., 1979, Données géologiques et radiométriques sur la mise en place de la Tellerteba (Hoggar): Colloquium of African Geology, 10th, Montpellier, France, Abstracts, p. 143.

Rougier, S., 2012, Interaction lithosphère-asthénosphère et mouvements verticaux: le cas du massif du Hoggar [Ph. D. thesis]: Université Paris-Sud, 277 p.

Rougier, S., Missenard, Y., Gautheron, C., Barbarand, J., Zeyen, H., Pinna, R., Liégeois, J.-P., Bonin, B., Ouabadi, A., and Derder, M. E.-M., Frison de Lamotte, D., 2013, Eocene exhumation of the Tuareg Shield (Sahara Desert, Africa): Geology, v. 41, p. 615-618.

Sandvol, E., Seber, D., Barazangi, M., Vernon, F., Mellors, R. , and Al-Amri, A., 1998, Lithospheric seismic velocity discontinuities beneath the Arabian Shield: Geophysical Research Letters, v. 25, p. 2873-2876.

Sebai, A., Stutzmann, E., Montagnera, J.-P., Sicilia, D., and Beuclerc, E., 2006, Anisotropic structure of the African upper mantle from Rayleigh and Love wave tomography: Physics of the Earth and Planetary Interiors, v. 155, p. 48–62

Shankland, T. L., and Ander, M., 1983, Electrical conductivity, temperatures and fluids in the lower crust: Journal of Geophysical Research, v. 88, p. 9475-9484.

Swift C. M. Jr., 1967, A Magnetotelluric Investigation of an Electrical Conductivity Anomaly in the Southwestern United States [Ph. D. thesis]: Massachusetts Institute of Technology, 223 p.

Tikhonov, A. N., 1950, Determination of electrical characteristics of the deep strata of the earth's crust: Doklady Akademii Nauk, v. 73, p. 292-297.

Unsworth, M. J., Egbert, G., and Booker, J., 1999, High-resolution electromagnetic imaging of the San Andreas fault in Central California: Journal of Geophysical Research, v. 105, p. 1131-1150.

Wannamaker, Ph. E., Hasterok, D. P., Johnston, J. M., Stodt, J. A., Hall, D. B., Sodergren, T. L., Pellerin, L., Maris, V., Doerner, W. M., Groenewold, K. A., and Unsworth, M. J., 2008, Lithospheric

dismemberment and magmatic processes of the Great Basin–Colorado Plateau transition, Utah, implied from magnetotellurics, Geochemistry, Geophysics, Geosystems, 9, Article number Q05019.

Wu, X., Ferguson, I. J., and Jones, A. G., 2002, Magnetotelluric response and geoelectric structure of the Great Slave Lake shear zone: Earth and Planetary Science Letters, v. 196, p. 35-50.